JJEE

Volume 11 | Number 1 | March 2025 | Pages 52-65

Jordan Journal of Electrical Engineering

ISSN (print): 2409-9600, ISSN (online): 2409-9619

Homepage: jjee.ttu.edu.jo

Indoor Multi-Different-Wall Path Loss Prediction Model Using Adaptive Neuro-Fuzzy Inference System

Shwan Ch. Abdulla[1*]

[1] Computer Engineering Department, College of Engineering, University of Sulaimani, Sulaymaniyah, Iraq
E-mail: shwan.abdullah@univsul.edu.iq

Received: May 24, 2024 *Revised: Jul 23, 2024* *Accepted: Jul 31, 2024* *Available online: Sep 25, 2024*

***Abstract*—** The efficiency of wireless systems is heavily dependent on the precision of the propagation channel model. Accurate prediction of signal path loss is an essential process in planning and optimizing radio networks. In this paper, a new indoor path loss prediction model - utilizing the Adaptive Neuro-Fuzzy Inference System (ANFIS) approach - is proposed. The proposed model takes into consideration the effect of different indoor barriers or wall types, in addition to other essential factors, on the propagation channel to obtain precise prediction in buildings with hybrid walls or partitions. On-site recorded WiFi data is used to build and verify the proposed model. To minimize modeling errors, a hybrid training method is employed, and the input membership functions of the model are optimized. The proposed ANFIS model is compared with the Cost-231 propagation model after it has been calibrated using a multilinear regression approach. The comparison indicates the superiority of the proposed model in terms of precision and accuracy. The obtained results show that the new model has a lower root mean square error and standard deviation with a higher correlation factor of 98%. The proposed ANFIS model produces precise indoor WiFi prediction and promotes accurate forecasting of other frequency bands - such as UMTS and GSM - in buildings with different interior structures.

***Keywords*—** ANFIS model; Path loss prediction; Multi-wall model; Indoor wave propagation; WiFi Model.

1. INTRODUCTION

Presently, there is an ongoing growth in the number of radio network subscribers with the desired services, which prompts the development of radio networks with the highest levels of quality of service. The operators must ensure sufficient signal strength in every region that the network covers, particularly in interior environments. For this reason, precise indoor propagation models have become necessary for radio network planning in order to accurately estimate the received power at every point along the path of the radio signal.

Generally, the radio wave in wireless networks undergoes three kinds of waste on its route to the reception point. These are the fading effect, shadow fading, and path-loss [1]. One of the most demanding tasks in the design of radio systems has been modeling the channel between the transmitter (TX) and the receiver (RX) of the wireless networks [2]. As a result, a variety of research projects have concentrated on developing various propagation and path-loss prediction models in different environments [3-6]. These models are classified into two types: deterministic models and empirical models. Deterministic models, such as frequency domain per flow [7] ray tracing [8], theory of diffraction [9] are more generic and efficient than empirical types; however, computationally demanding since they require comprehensive environmental information. While empirical models are simpler and rely on received power measurements and statistical distributions of the environment [10-12].

* Corresponding author

DOI: https://doi.org/10.5455/jjee.204-1716561420

In practice, the raw received signal strength (RSS) data of indoor wireless signals, sent by a TX to an RX, is invariant with time and stochastic. The indoor environment's elements; such as doors, different wall types, and other obstacles, explain such stochasticity and temporal propagation changes. Consequently, utilizing an intelligent propagation model that accurately mimics the characteristics of the signal becomes essential. Furthermore, obtaining signal strength data for all the constructions without performing radio surveys would be both time-efficient and cost-effective.

To cope with stochastic variations in wireless signals and overcome inaccuracies in the path-loss prediction models, artificial intelligence (AI) techniques can be employed [13-17]. This is due to the fact that AI is adaptable and is based on empirical information rather than the analytical calculations of a system. The ANFIS is a highly effective method for modeling complex and nonlinear systems with small training data and high precision [18-20]. It combines fuzzy systems and neural networks in such that the neural network is utilized to regulate and automatically tune the fuzzy system's parameters [21].

In the literature, there are few attempts to use the ANFIS approach for indoor path loss prediction [22-24]. Those approaches predict the decrease in RSS without taking into consideration the attenuation resulting from some essential factors, such as a combination of different sizes or types of walls existing on the same floor, which increases the prediction error in buildings with hybrid walls or partitions. Also, these studies do not consider the effect of different design parameters, such as the number and type of membership functions used per input, which may decrease the precision of the model. For this reason, it is feasible to lower the range of error for indoor wireless systems by correctly selecting the inputs and the design parameters of the model to obtain a precise signal prediction.

In this paper, the ANFIS approach is adopted to build a precise propagation model to predict the path loss of a received indoor Wi-Fi signal. The model takes into consideration the distance (D) between the TX and RX, the number (Wn) and type (Wt) of walls penetrated by the signal and the frequency (F) of the signal. On-site measured data is used to create and verify the ANFIS model. Also, a study was conducted to select the appropriate number and type of membership function for each input of the model to minimize modeling errors and increase the precision and accuracy of the model. The performance of the proposed model is analyzed and compared with a widely used Cost-231 multi-wall propagation model after calibration using multiple linear regression approaches as performance metrics.

The remainder of this research paper is organized as follows: Section 2 describes the multi-wall propagation model. Section 3 explains the experimental setup and on-site measurements. Section 4 introduces detailed information about ANFIS architecture and modeling. Section 5 describes the design, performance and reusability of the proposed ANFIS propagation model. A comparison between the proposed ANFIS model with the MW model, after calibration, is introduced in section 6. Finally, the conclusion is presented in section 7.

2. THE MULTI-WALL PROPAGATION MODEL

For radio wave propagation, numerous empirical models were created [25]. They can be classified into two different types: general-site and site-specific models [26]. The most accurate and widely used propagation model is the Cost 231 Multi-Wall (MW) model, as it accounts for losses related to the environment, such as walls [27-30]. The fundamental idea behind the MW representation is to anticipate the path loss of the signal, and its accuracy is correlated with the accuracy of walls and floors attenuation estimates. Based on the ray-tracing theory, the MW model considers the nonlinear relationship between the total attenuation and the number of traversed walls or floors. The MW model is expressed as [30]:

$$L_d[dB] = L(d_o) + 10nlog(d) + \sum_{i=1}^{I} \sum_{k=1}^{K_{wi}} L_{wik} + \sum_{j=1}^{J} \sum_{k=1}^{K_{fj}} L_{fjk} \quad (1)$$

where: L_d represents the path loss at distance (d) in dB, $L(d_o)$ represents the path loss at 1m distance, n is the path loss index, which is determined as 1.96 in the free space, d is the distance between the transmitter and receiver, L_{wik} is the attenuation due to penetrating K^{th} walls of type i, L_{fjk} is the attenuation due to penetrating K^{th} floors of type j, I and J represent the number of penetrated walls and floors respectively, K_{fj} is the number of floor types j, K_{wi} is the number of wall types i.

This model will be utilized in subsequent sections for comparison purposes to evaluate the performance and accuracy of the newly proposed ANFIS model for indoor path loss prediction.

3. MEASUREMENT CAMPAIGN

The availability of precise samples is crucial to creating a generic site model and ensuring model reliability. To successfully achieve this objective, the AutoCad software is used to depict the measuring environment together with Netstumbler software for precise wireless signal detection. Data collection is conducted on the second floor of the General Eye Hospital in Sulaymaniyah city, Iraq. The floor of the building is constructed of two types of walls: 20cm and 12cm concrete block walls [31]; hence, the attenuation due to these two different wall types is taken into consideration using the developed model.

The measurements are conducted using a TX and a RX unit. The transmitter is represented by the D-Link AirPlus Xtreme G _DWL-2100AP unit which is a 802.11g wireless access point device that operates at the 2.4-2.4835Ghz frequency range. It provides a signal strength of 31mw, i.e.15 dBm, using a dipole antenna of 2 dB antenna gain. The receiver unit is represented by a Dell Inspiron Laptop equipped with a Dell Wireless 1395 WLAN card which works at a frequency of 2.4Ghz using the IEEE 802.11b standard. Netstumbler software is employed to detect and record the signal received by the WLAN card. The received signal strength alters from -92 to -30 dB m, within a variable range of approximately 62 dB.

A room located at the center of the floor is used for the TX. It is 6.8m x 6.8m width and 3m height with gypsum board secondary ceiling. It has a 2m x 2.5m auxiliary room. The TX is placed on a table of 1m height while the RX, i.e. the laptop, is located on another table at the same TX height. The locations of measurements are chosen to ensure both line of sight (LOS) and non-line of sight (NLOS) scenarios. The measurement of the signal is conducted, with steps of 18°, starting from 0° to 180°, every 1m around the TX position. This scenario is repeated in a straight line to cover all other rooms available on the floor. Fig. 1 shows the TX position and the different locations of the receiver, denoted by small circles, where the measurements are conducted. To ensure accurate measurements, the Lee criterion [32] is taken into consideration, which emphasizes that a mean from at least 50 samples, from a signal separated by 40 wavelengths, must be taken to achieve a 90% confidence interval. For this reason, over a period of 60 seconds, 60 samples of the received power are recorded for each location of the receiver. The 60 samples of each location are averaged to balance out the effect of fading due to obstacle movement, i.e. people, or time delay variations. Finally, a total of 170 values of different locations are obtained and used to build the model, as explained in subsequent sections.

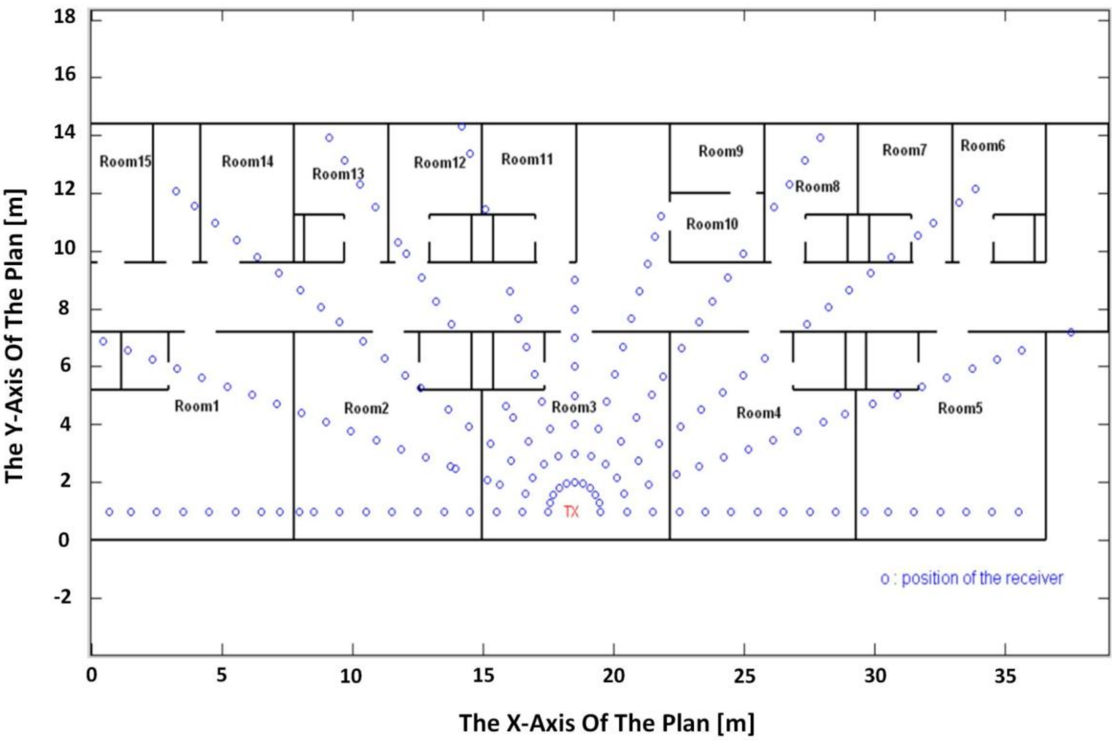

Fig. 1. The floor plan with the transmitter (TX) and different receiver positions [31].

4. ADAPTIVE NEURO-FUZZY INFERENCE SYSTEM (ANFIS)

Numerous nonlinear real-world problems have been solved using AI paradigms, including fuzzy logic inference, evolutionary algorithms and neural networks [33-36]. The ability of a Fuzzy Logic System (FLS) to describe nonlinear input-output relationships, by a set of if-then rules, is one of its key benefits. On the other hand, the fundamental benefit of an Artificial Neural Network (ANN) is the built-in learning ability that allows the networks to adaptively enhance their performance. The adaptive and precise learning capacities of neural networks, along with the generalization and quick learning abilities of FLS, are the main characteristics of neuro-fuzzy networks. The neuro-fuzzy system, which combines the advantages of rule-based fuzzy systems with the learning capabilities of neural networks, can dramatically enhance performance and offer a method for integrating prior observations into the classification process. In artificial neural networks, the training process effectively creates the system, while a neuro-fuzzy network uses fuzzy logic principles to build the system, and then refines it using neural network training techniques.

4.1. ANFIS Architecture

ANFIS is a neuro-fuzzy model framework that adjusts itself through learning. ANFIS is a fuzzy logic inference system that uses a five-layer feed-forward network as its architecture. The five layers that make up the ANFIS system architecture are: the fuzzy layer, the product layer, the normalization layer, the de-fuzzy or consequent layer, and the overall output layer. Fig. 2 illustrates the ANFIS architecture, which consists of two inputs, one output, and two rules. In this linked structure, the squares indicate adaptive node functions, while the circles represent fixed node functions. The nodes in the hidden layers serve as membership functions and rules, while the input and output nodes reflect the training values and the predicted values, respectively.

To help comprehend ANFIS, two if-then rules of a first order Sugeno fuzzy inference system are considered here:

$Rule$ 1: $If\ x\ is\ A_1\ and\ \ y\ is\ B_1\ \ then\ \ \ f\ = p_1\, x\ +\ q_1 y\ +\ r_1$

$Rule$ 2: $If\ x\ is\ A_2\ and\ \ y\ is\ B_2\ \ then\ \ \ f\ = p_2\, x\ +\ q_2 y\ +\ r_2$

Also, in terms of membership degrees, the aforementioned rules can also be written as:

$Rule$ 1: $If\ \mu_{A_1}(x)\ \ and\ \ \mu_{B_1}(y)\ \ then\ \ \ f\ = p_1\, x\ +\ q_1 y\ +\ r_1$

$Rule$ 2: $If\ \mu_{A_2}(x)\ \ and\ \ \mu_{B_2}(y)\ \ then\ \ \ f\ = p_2\, x\ +\ q_2 y\ +\ r_2$

where A_i and B_i are the membership functions, and p_i, q_i, and r_i represent the parameters of fuzzy rules' consequent part. The nodes of membership functions layer (layer 1) and the consequent layer (layer 4) are adjustable, while the nodes of the product layer (layer 2) and normalization layer (layer 3) are unchangeable. The five layers of ANFIS structure are explained as the following:

- **Layer 1:** known as the fuzzy layer. A parameterized membership function, such as a Gaussian, Trapezoidal, Generalized Bell or Triangle function, makes up each node i of this layer. Premised parameters are the term used to describe the parameters of membership functions.

$$O_{i,1} = \mu_{A_i}(x), \quad for\ \ i = 1,2$$
$$O_{i,1} = \mu_{B_{i-2}}(x), \quad for\ \ i = 3,4 \tag{2}$$

where x represents the input to node i, while O_i represents the membership function degree of the input x in a fuzzy set A_i. The generalized bell membership function is a frequently utilized method to define fuzzy sets due to their clear notation and smoothness. It is defined as:

$$\mu_{A_i}(x) = \frac{1}{1+\left|\frac{x-c_i}{a_i}\right|^{2b_i}} \tag{3}$$

where a_i, b_i, $and\ c_i$ represent the parameters of the membership function and known as premised parameters. By adjusting a_i and c_i, the membership function's center and width can be modified. The slopes at the crossover areas are determined by the parameter b_i. The premised parameters are tuned during the learning process of ANFIS. The preceding segments of fuzzy rules, i.e. IF part, are formed by this layer.

- **Layer 2:** known as the product layer. It consists of fixed nodes that each have a single fuzzy rule. The output, which indicates the firing strength of each rule, is the product of all incoming signals.

$$O_{2,i} = w_i = \mu_{A_i}(x)\,\mu_{B_i}(y), \quad for\ \ i = 1,2 \tag{4}$$

Using grid partitioning, the automatically generated rules are m^n, where m is the number of membership functions in each input and n represents the entire number of inputs.

- **Layer 3:** Known as normalization layer. The nodes in this layer are all fixed nodes. The i_{th} node determines the ratio of the firing strength of the i_{th} rule to the total firing strength of all rules. In this layer, each node produces a normalized firing strength of a rule as:

$$O_{3,i} = \overline{w}_i = \frac{w_i}{w_1+w_2}, \quad for\ i = 1,2 \tag{5}$$

where $\overline{w}_i$, w_i , w_1 and w_2 are the i_{th} rule's normalized firing strength, the i_{th} rule's firing strength, the first rule's firing strength and the second rule's firing strength, respectively.

- **Layer 4:** Known as the consequent layer. In this layer, each node is adaptable and represents the consequent section, i.e. THEN part, of a fuzzy rule using node function $f_i = p_i x + q_i y + r_i$, as:

$$O_{4,i} = \overline{w}_i f_i = \overline{w}_i(p_i x + q_i y + r_i) \tag{6}$$

where $\overline{w}_i$ is the i_{th}rule's normalized firing strength, and $\{p_i, q_i, r_i\}$ are linear parameters of the consequent part of the i_{th} fuzzy rule. During the training of ANFIS, the parameters $\{p_i, q_i, r_i\}$ are determined.

- **Layer 5:** Known as summation layer. This layer has one fixed node that determines the final output by summing all incoming signals.

$$O_{5,i} = \sum_{i=1}^{2} \overline{w}_i f_i = \frac{\sum_{i=1}^{2} w_i f_i}{w_1 + w_2} \tag{7}$$

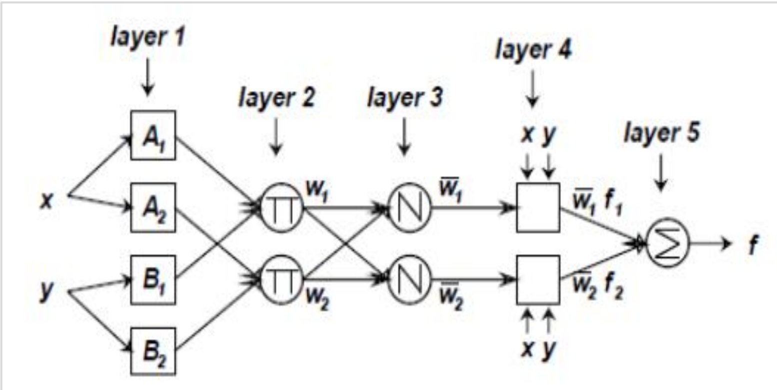

Fig. 2. ANFIS architecture [18].

4.2. ANFIS Learning Algorithm

The objective of the learning algorithm for the mentioned ANFIS architecture is to adjust the adaptable parameters, i.e. $\{a_i, b_i, c_i\}$ and $\{p_i, q_i, r_i\}$, to ensure that the ANFIS output resembles the training data. The output of the model can be described as follows when the membership function's premise coefficients $\{a_i, b_i, c_i\}$ are predetermined:

$$f = \frac{w_1}{w_1 + w_2} f_1 + \frac{w_2}{w_1 + w_2} f_2 \tag{8}$$

By substituting Eq. (5) into Eq. (8), it becomes:

$$f = \overline{w}_1 f_1 + \overline{w}_2 f_2 \tag{9}$$

By substituting the consequent part of the fuzzy rules into Eq. (9), it yields:

$$f = \overline{w}_1(p_1 x + q_1 y + r_1) + \overline{w}_2(p_2 x + q_2 y + r_2) \tag{10}$$

By re-arrangement, the output becomes:

$$f = (\overline{w}_1 x)\, p_1 + (\overline{w}_1 y)\, q_1 + (\overline{w}_1)\, r_1 + (\overline{w}_2\, x)\, p_2 + (\overline{w}_2\, y)\, q_2 + (\overline{w}_2)\, r_2 \tag{11}$$

It is clear that the output function is a combination of the adjustable consequent parameters $\{p_1, q_1, r_1\}$ and $\{p_2, q_2, r_2\}$. The optimal values of these coefficients can be simply obtained by using the least squares method. The search space grows larger, and the training's convergence slows down when the premise coefficients are not specified. This problem can be solved by using a hybrid approach that combines the gradient descent method and the least squares method. The hybrid algorithm consists of a forward and a backward pass. The forward pass is achieved when the premise coefficients are specified, and the consequent coefficients are optimized using the least squares approach. While the backward pass commences immediately after the optimal consequent coefficients are determined. The gradient descent approach (backward pass) is utilized to optimally modify the premise coefficients of the input domain's fuzzy sets. Utilizing the consequent parameters specified in the forward pass, the ANFIS output is computed while the output error of the ANFIS is employed by a conventional backpropagation technique to adjust the premise parameters. This hybrid approach is highly successful at training the ANFIS [18].

5. THE NEW INDOOR PROPAGATION MODEL

5.1. Design of the ANFIS Model

To create an accurate and reliable ANFIS model, the greatest number of effective parameters must be considered. In this work, the inputs of the designed ANFIS model are inspired by the MW reference model. These are: the distance (D) between the transmitter and the receiver, the frequency of the signal (F), the number of walls (Wn) and the type of walls (Wt) being penetrated by the signal to obtain the attenuation due to different wall types existing in the building. An illustration of the designed ANFIS model is shown in Fig. 3.

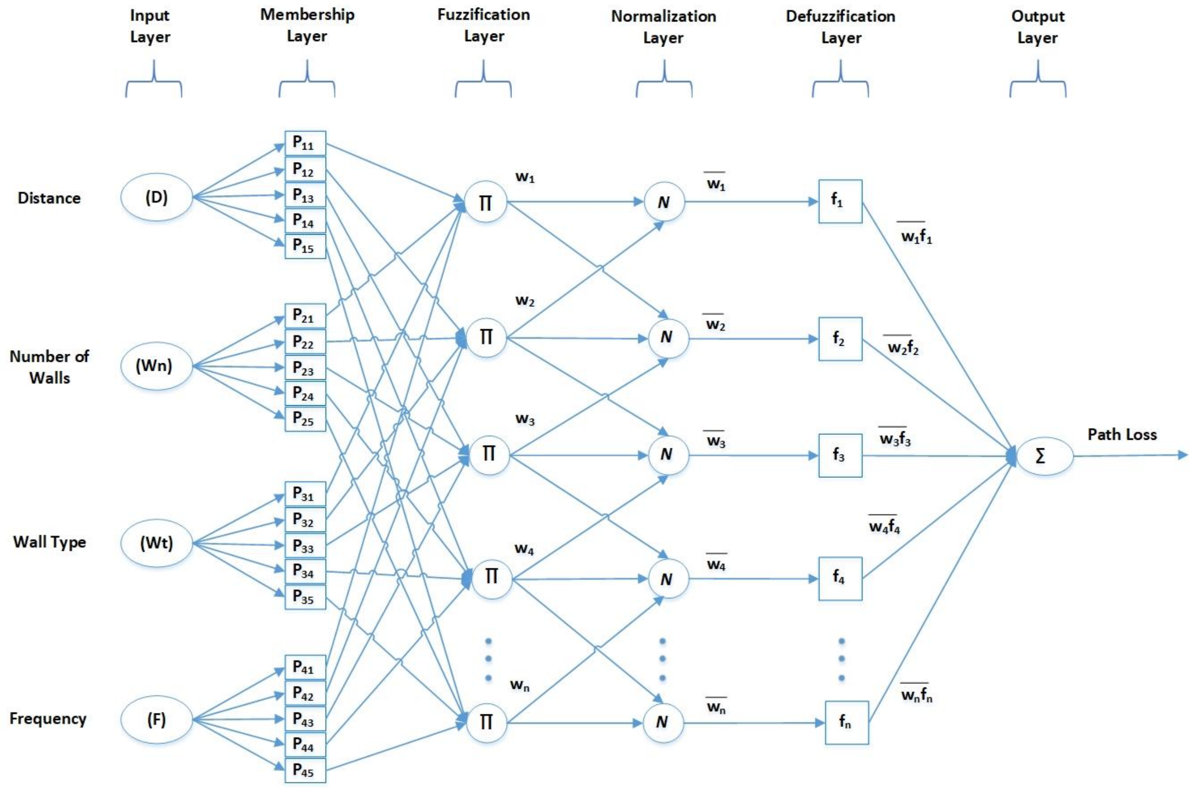

Fig. 3. The designed ANFIS model.

Tables 1-3 show the description and the range of each input of the model. It is important to mention that most of the buildings are constructed from different types of walls with different sizes and materials. Hence, it's essential for the model to consider different combinations of walls, that may encounter the signal while propagating from transmitter to receiver, to account for different attenuation values. For this reason, the proposed model considers various cases: whether the floor consists of a single type of walls, i.e. C1: Concrete 20cm, C2: Concrete 12cm, B1: Brick 20cm, or consists of a combination of different wall types, such as 2 x C1 + 1 x C2, as shown in Table 2. In this research, the measurements were taken in the General Eye Hospital building in Sulaymaniyah city, Iraq, at which the floor is constructed with two different types of walls, 20cm and 12cm concrete blocks. For this reason, the attenuation of these wall types is considered, as shown in Table 2 Index [7-9]. Table 3 shows the possible frequency bands that can be used by this model. However, in this work, only the 2.4GHz frequency band (WiFi) is employed. Table 2 and Table 3 can be extended to include more different wall combinations and frequency bands, respectively.

Table 1. ANFIS model input parameters.

Parameter	Description	Range
D	Distance between transmitter and receiver (in meters)	[1-50]
Wn	Number of Walls/Floors	[0-10]
Wt	Wall type/size	[0-10]
F	Frequency band	[1-3]

Table 2. Different combination of wall types/sizes penetrated by the signal during propagation.

Index	Description
0	No obstacle
1	C1: Concrete 20cm
2	C2: Concrete 12cm
3	B1: Brick 20cm
4	B2: Brick 40cm
5	S1: Stone
6	G1: Wood
7	1 x C1 + 1 x C2
8	2 x C1 + 1 x C2
9	1 x C1 + 2 x C2
10	1 x C1 + 2 x B2

Table 3. The frequency bands that can be used by the model.

Index	Frequency	Description
1	(2.4 – 2.48) GHz	WiFi
2	(1850 – 1990) MHz	GSM
3	(1920 – 2170) MHz	UMTS

In this research, the ANFIS toolbox provided by MATLAB 2020a software is used to create the ANFIS model. The architecture of the designed ANFIS model consists of four inputs and one output, with five generalized bell membership functions (Gbellmf) for each input. The reason behind selecting this number and type of membership function per input is explained in the next section. The number of Epochs is determined empirically and set to 200 to obtain the least RMSE value. Data classification is performed using the grid partition method and hybrid optimization approach to train the FIS. To create the model, on-site measured data of 170 values is divided into two sets. The first data set, which consists of 130 values, is used for training the model, while the second data set of the remaining 40 values is used for model verification.

5.1.1 *Selection of Input Membership Function*

In this section, to increase the precision and obtain an accurate ANFIS model, the effect of the type and the number of membership functions per input is studied. During the training phase of the model, the simulation is repeated to test eight different membership functions with different numbers of functions per input. The resultant modeling error, i.e. RMSE, is recorded as shown in Table 4.

It is clear from Table 4 that by using the gaussian2 (Gauss2mf) or the generalized bell (Gbellmf) membership functions, the model performs better as the error is less, compared to other options. Also, increasing the number of membership functions per input leads to decrease the RMSE of the model. Hence, in this work, to obtain a precise model, five generalized bell membership functions (Gbellmf) are used for each input. This will lead to a model of minimal RMSE which can be interpreted as better replication of the measured data and promote a more accurate model as compared to other options.

Table 4. The RMSE values during the training of ANFIS model using different membership functions.

No. of MF/Input	Trimf	Trapmf	Gbellmf	Gaussmf	Gauss2mf	Pimf	Dsigmf	Psigmf
2	3.41	3.44	3.40	3.38	3.44	3.49	3.40	3.40
3	2.94	3.02	2.90	2.88	2.90	3.04	2.96	2.96
4	2.95	2.88	2.82	2.85	2.84	2.89	2.85	2.85
5	2.80	2.89	2.71	2.83	2.73	2.89	2.85	2.85
6	2.80	2.87	2.71	2.80	2.73	2.89	2.82	2.82

5.2 Model Performance and Reusability

After the learning phase, the ANFIS model must emulate the behavior of the system so that predicted values match the measured values as accurately as possible. The performance of the ANFIS model can be seen in Fig. 4, which shows the response of the ANFIS model at the learning phase in comparison with the measured data.

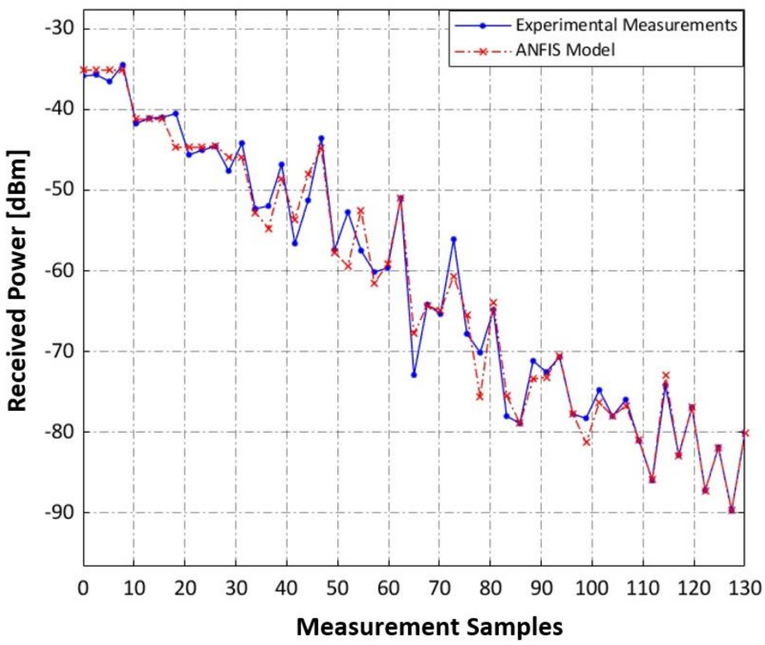

Fig. 4. Response of the ANFIS model during learning process.

To test the reusability of the model, the developed and trained model is tested with the second data set of measurements that was not used during the learning process. This comparison is shown in Fig. 5.

According to statistics applied to measured error, error = predicted – measured value, the mean error (ME) is 4.94E-06, and the standard deviation (SD) is around 2.74 dB. The results obtained indicate that the proposed model offers highly precise prediction of indoor signal propagation and complies with an ITU requirement that indoor models with a mean error close to zero and an error standard deviation less than 8 dB [37] can be regarded as accurate. Another parameter, called the correlation factor, can be utilized to support the results more strongly.

The interdependence between the measured and estimated values is measured by this parameter. A high correlation coefficient indicates that measurements and predicted values correspond. A low score indicates that the measurements and prediction are unrelated, which implies that the prediction is unable to accurately reflect the actual measurements' behavior. The calculated correlation factor between prediction and measurements shows a high correlation value of about 98%.

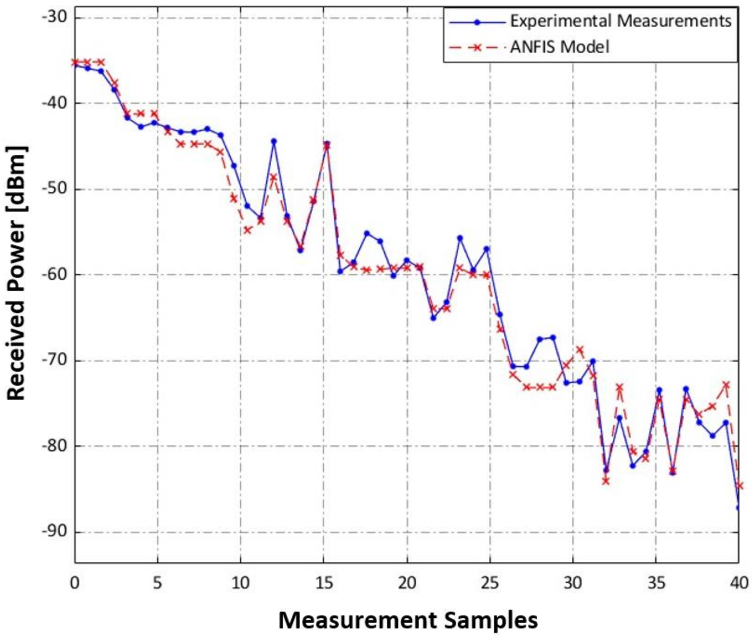

Fig. 5. Comparison between real measurements and ANFIS model prediction.

6. COMPARISON BETWEEN THE MW AND ANFIS MODELS

In this section, a performance comparison between the MW model and the new proposed ANFIS model is presented to emphasize the benefits of the new model over the existing model. The comparison can only be performed after the calibration of the MW model. A multiple linear regression method is used for model calibration. The attenuation of the signal can be expressed as [38]:

$$L_i = A + B * log_{10}(d_i) + C + D \tag{12}$$

where $A = L(d_o)$; $B = 10n$; $C = p * L_{wik}$ and $D = q * L_{fjk}$. Also, L_i represents the path loss at distance (d_i), $L(d_o)$ is the path loss at a distance of 1m, n is the path loss index, d_i is the distance between TX and RX, L_{wik} is the attenuation due to traversed wall of type i, L_{fjk} is the attenuation due to traversed floor of type j.

Knowing that p represents the number of walls being moved across by the signal from the TX to the RX; q represents the number of floors being moved across by the signal from the TX to the RX (in this research, this number equals zero since a single floor was taken into consideration); L_{mes} represents the measured attenuation at the same distance; For a single sample, L_i can be expressed as:

$$L_i = (1, log_{10}(d_i), 1, 1) * \begin{pmatrix} A \\ B \\ C \\ D \end{pmatrix} \quad (13)$$

For N different samples, Eq. (13) can be expressed in a reduced form as:

$$L_i = M * Y \quad (14)$$

where: $L_i = \begin{pmatrix} L(d_1) \\ L(d_2) \\ \vdots \\ L(d_n) \end{pmatrix}$, $M = \begin{pmatrix} 1, log_{10}(d_1), 1, 1 \\ 1, log_{10}(d_2), 1, 1 \\ \vdots \\ 1, log_{10}(d_n), 1, 1 \end{pmatrix}$ and $Y = \begin{pmatrix} A \\ B \\ C \\ D \end{pmatrix}$.

To minimize the error between the measured and the predicted (~) values, the equation of error is expressed as:

$$e = L_{mes} - M * \tilde{Y} \quad (15)$$

For optimal values of $\tilde{Y}$, the error equals zero and hence we obtain:

$$M^t * \left(L_{mes} - M * \tilde{Y}_{opt}\right) = 0 \quad (16)$$

Together with:

$$\tilde{Y} = (M^t * M)^{-1} * M^t * L_{mes} \quad (17)$$

Finally, using the optimal values, the attenuation is calculated as:

$$L_i = \tilde{A} + \tilde{B} * log_{10}(d_i) + \tilde{C} + \tilde{D} \quad (18)$$

Table 5 and Fig. 6 present a comparison of the predicted values, obtained from the calibrated MW model and the new ANFIS model, with the measured values.

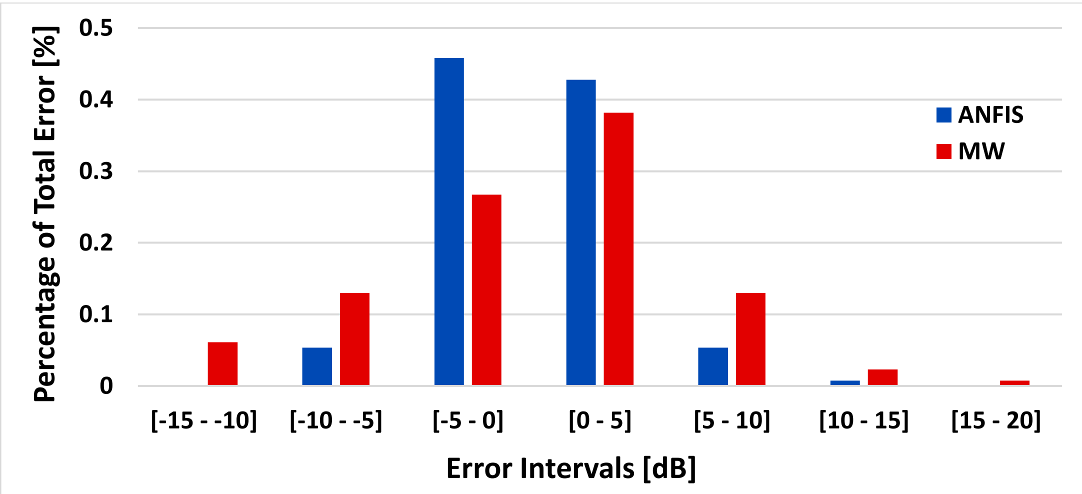

Fig. 6. Error distribution of the ANFIS and MW models.

As depicted in Fig. 6, it can be inferred that the ANFIS model prediction histogram tracks the trend of measured data more closely than the MW model. The statistics in Table 5 provide further proof of these results as the ANFIS model displays a lower RMSE of 2.7302 dB and a lower SD of 2.7407 with a higher correlation factor of about 98%. These results can be interpreted by the fact that the calibration of the MW model is achieved by estimating the wall attenuation factors using a multi-linear regression method which assumes a linear model with uncorrelated variables. The error distribution of the two models is shown in Fig. 6 to support the results that were obtained. This statistic, which shows the percentage of errors that occur within a specific interval, is utilized to confirm the accuracy of the model. The greatest number of errors must be almost equal to zero in order for a model to be accurate.

The histogram of Fig. 6 shows the high performance of the ANFIS model as the distribution of error beyond ±5dB is approximately 11%, while the distribution for the MW model is nearly 35%. Such results confirm the precision and accuracy of the proposed ANFIS model.

Table 5. Comparison between the ANFIS and the MW models.

Parameter	ANFIS	MW
RMSE	2.7302	5.9632
SD	2.7407	5.9860
Correlation Factor	0.9859	0.9306

7. CONCLUSIONS

In this research, an indoor multi-different-wall WiFi path loss prediction model was presented. The model was built with the aid of the adaptive neuro-fuzzy inference system (ANFIS) method. The model takes into consideration the distance between transmitter and receiver, the number and different types of walls being penetrated by the signal and the signal frequency. On-site measured data was used to create and verify the model. The performance of the proposed model was compared with that of a well-known multi-wall propagation model. The results show that the proposed model surpasses the multi-wall model in terms of Root Mean Square Error (RMSE), Standard Deviation (SD) and correlation factor (98%). This is due to the fact that the ANFIS model is adaptive and has the ability to deal with dynamic changes in the environment with high accuracy. The proposed model offers a high prediction of indoor propagation with a mean error of 4.94E-06 dB and a standard deviation of 2.74 dB. This complies with an ITU requirement that indoor models with a mean error close to zero and a standard deviation less than 8 dB [37] can be regarded as accurate. Hence, the proposed ANFIS model is precise and promotes accurate indoor Wi-Fi signal prediction in buildings with different types of interior partitions. The designed model can be utilized for the prediction of other frequency bands, such as UMTS and GSM.

REFERENCES

[1] T. Rappaport, *Wireless Communications: Principles and Practice*, Prentice Hall, 2001.

[2] B. Amer, A. Noureldin, "Modeling received signal strength for indoors utilizing hybrid neuro-fuzzy network," 7th International Conference on Modeling, Simulation, and Applied Optimization, 2017, doi: 10.1109/ICMSAO.2017.7934848.

[3] R. Akl, D. Tummala, X. Li, "Indoor propagation modeling at 2.4 GHz for IEEE 802.11 networks," *wireless and optical communications*, 2006.

[4] K. Cheung, J. Sau, R. Murch, "A new empirical model for indoor propagation prediction," *IEEE transactions on Vehicular Technology*, vol. 47, no. 3, pp. 996-1001, 1998, doi: 10.1109/25.704854.

[5] O. Ata, A. Shahateet, M. Jawadeh, A. Amro, "An indoor propagation model based on a novel multi wall attenuation loss formula at frequencies 900 MHz and 2.4 GHz," *Wireless Personal Communications*, vol. 69, no.1, pp. 23-36, 2013, doi: 10.1007/s11277-012-0558-x.

[6] C. Lim, J. Volakis, K. Sertel, R. Kindt, A. Anastasopoulos, "Indoor propagation models based on rigorous methods for site-specific multipath environments," *IEEE Transactions on Antennas and Propagation*, vol. 54, no. 6, pp. 1718-1725, 2006, doi: 10.1109/TAP.2006.875493

[7] G. Roche, J. Gorce, "A 3D formulation of MR-FDPF for simulating indoor radio propagation," First European Conference on Antennas and Propagation, 2006, doi: 10.1109/EUCAP.2006.4584787.

[8] M. Sarker, A. Reza, K. Dimyati, "A novel ray-tracing technique for indoor radio signal prediction, " *Journal of Electromagnetic Waves and Applications*, vol. 25, no. 8-9, pp. 1179-1190, 2011, doi: 10.1163/156939311795762222.

[9] M. Jacob, S. Priebe, R. Dickhoff, T. Kleine-Ostmann, T. Schrader, T. Kurner, "Diffraction in mm and sub-mm wave indoor propagation channels," *IEEE Transactions on Microwave Theory and Techniques*, vol. 60, no. 3, pp. 833-844 , 2012, doi: 10.1109/TMTT.2011.2178859

[10] Y. Solahuddin, R. Mardeni, "Indoor empirical path loss prediction model for 2.4 GHz 802.11n network," IEEE International Conference on Control System, Computing and Engineering, 2011, doi: 10.1109/ICCSCE.2011.6190487.

[11] A. Zyoud, J. Chebil, M. Habaebi, M. Islam, A. Zeki, "Comparison of empirical indoor propagation models for 4G wireless networks at 2.6 GHz," *Proceedings Engineering & Technology*, vol. 3, pp. 7-11, 2013.

[12] A. Sandeep, Y. Shreyas, S. Seth, R. Agarwal, G. Sadashivappa, "Wireless network visualization and indoor empirical propagation model for a campus wi-fi network," *World Academy of Science, Engineering and Technology*, vol. 42, pp. 730-734, 2008.

[13] H. Jo, C. Park, E. Lee, H. Choi, J. Park, "Path loss prediction based on machine learning techniques: principal component analysis, artificial neural network, and Gaussian process," *Sensors*, vol. 20, no. 7, p. 1927, 2020, doi: 10.3390/s20071927.

[14] S. Ma, H. Cheng, H. Lee, "A practical approach to indoor path loss modeling based on deep learning," *Journal of Computing Science and Engineering*, vol. 15, no. 2, pp. 84-95, 2021.

[15] M. Elmezughi, O. Salih, T. Afullo, K. Duffy, "Comparative analysis of major machine-learning-based path loss models for enclosed indoor channels," *Sensors*, vol. 22, no. 13, pp. 4967, 2022, doi: 10.3390/s22134967.

[16] S. Aldossari, "Predicting path loss of an indoor environment using artificial intelligence in the 28-GHz band," *Electronics*, vol. 12, no. 3, pp. 497, 2023, doi: 10.3390/electronics12030497.

[17] H. Singh, S. Gupta, C. Dhawan, A. Mishra, "Path loss prediction in smart campus environment: machine learning-based approaches," IEEE 91st Vehicular Technology Conference, 2020, doi: 10.1109/VTC2020-Spring48590.2020.9129444.

[18] K. Yavarian, F. Hashemi, A. Mohammadian, "Design of intelligent PID controller for AVR system using an adaptive neuro fuzzy inference system," *International Journal of Electrical and Computer Engineering*, vol. 4, no. 5, pp. 703-718, 2014.

[19] C. Voloşencu, *Introductory Chapter: ANFIS for Modeling Multivariable Nonlinear Functions*, IntechOpen, 2024. doi: 10.5772/intechopen.111237.

[20] K. Zergaw, M. Tuka, "Analysis of voltage dip impact on doubly fed induction generator under dynamic conditions," *Jordan Journal of Electrical Engineering*, vol. 9, no. 3, p. 338-356, 2023, doi: 10.5455/jjee.204-1669034454.

[21] J. Jang, "ANFIS: adaptive-network-based fuzzy inference system," *IEEE transactions on systems, man, and cybernetics*, vol. 23, no. 3, pp. 665-685, 1993, doi: 10.1109/21.256541.

[22] M. Omae, E. Ndungu, P. Kibet, "Wi-Fi Signal Indoor LOS Coverage modeling using ANFIS," Proceedings of the Sustainable Research and Innovation Conference, 2016.

[23] O. Bashorun, O. Shoewu, W. Alao, L. Oborkhale, N. Salau, "Analysis and prediction of indoor wireless propagation using adaptive neuro-fuzzy inference system," *The Pacific Journal of Science and Technology*, vol. 18, no. 2, pp. 155-162, 2017.

[24] Z. Adeyemo, T. Olawuyi, O. Oseni, S. Ojo, "Development of a path-loss prediction model using adaptive neuro-fuzzy inference system," *International Journal of Wireless and Microwave Technologies*, vol. 9, no. 6, pp. 40-53, 2019, doi: 10.5815/ijwmt.2019.06.05.

[25] E. Damosso, L. Correia, DGX III Commission, "COST action 231: digital mobile radio towards future generation system: final report," *European Commission,* Brussels, 1999, https://op.europa.eu/en/publication-detail/-/publication/f2f42003-4028-4496-af95-eaa38fd475f.

[26] A. Zineb, M. Ayadi, "A multi-wall and multi-frequency indoor path loss prediction model using artificial neural networks," *Arabian Journal for Science and Engineering*, vol. 41, no. 3, pp. 987-996, 2016, doi: 10.1007/s13369-015-1949-6.

[27] G. Caso, L. Nardis, "Virtual and oriented WiFi fingerprinting indoor positioning based on multi-wall multi-floor propagation models," *Mobile Networks and Applications*, vol. 22, pp. 825-833, 2017, doi: 10.1007/s11036-016-0749-x.

[28] M. Klepal, D. Pesch, "Influence of predicted and measured fingerprint on the accuracy of RSSI-based indoor location systems," IEEE 4th Workshop on Positioning, Navigation and Communication, 2007, doi: 10.1109/WPNC.2007.353626.

[29] A. Borrelli, C. Monti, M. Vari, F. Mazzenga, "Channel models for IEEE 802.11b indoor system design," 2004 IEEE International Conference on Communications, vol. 6, 2004, doi: 10.1109/ICC.2004.1313233.

[30] M. Lott, I. Forkel, "A multi-wall-and-floor model for indoor radio propagation," IEEE VTS 53rd Vehicular Technology Conference, 2001, doi: 10.1109/VETECS.2001.944886.

[31] A. Sulaiman, “Wireless network simulation and modelling of indoor radio wave propagation for radio coverage maps,” University of Sulaimani, MSc dissertation, 2010.

[32] G. Evans, B. Joslin, L. Vinson, B. Foose, "The optimization and application of the WCY Lee propagation model in the 1900 MHz frequency band," IEEE 47th Vehicular Technology Conference. Technology in Motion, 1997, doi: 10.1109/VETEC.1997.596324.

[33] J. Ren, Y. Zhu, Y. Zhang, D. Li, "Optimization of multi-receiver SNRs for indoor visible light communication based on modified evolutionary algorithm," *Optik*, vol. 228, pp. 166158, 2021, doi: 10.1016/j.ijleo.2020.166158.

[34] M. Saleem, M. Khan, S. Abbas, M. Asif, M. Hassan, J. Malik, "Intelligent FSO link for communication in natural disasters empowered with fuzzy inference system," IEEE International Conference on Electrical, Communication, and Computer Engineering, 2019, doi: 10.1109/ICECCE47252.2019.8940752.

[35] S. Yordanova, M. Slavov, "Stability analysis of model-free adaptive fuzzy logic control system applied for liquid level control in soda production, " *Jordan Journal of Electrical Engineering*, vol. 9, no. 1, pp. 14-30, 2023, doi: 10.5455/jjee.204-1667497864.

[36] M. Lee, G. Yu, H. Dai, "Decentralized inference with graph neural networks in wireless communication systems," *IEEE Transactions on Mobile Computing*, vol. 22, no. 5, pp. 2582–2598, 2021, doi: 10.1109/TMC.2021.3125793.

[37] P. Series, "Propagation data and prediction methods for the planning of indoor radio communication systems and radio local area networks in the frequency range 900 MHz to 100 GHz," *Recommendation ITU-R, P.1238-7*, 2012, https://www.itu.int/rec/R-REC-P.1238.

[38] M. Ayadi, S. Tabbane, Z. Belhaj, "Calibration of propagation model for indoor Tunisian environment," 3rd International Conference: Sciences of Electronic, Technologies of Information and Telecommunications, 2005.